Manuscript prepared for Atmos. Chem. Phys. Discuss.
with version 2014/09/16 7.15 Copernicus papers of the LaTeX class copernicus.cls.
Date: 27 August 2015

Diesel-related hydrocarbons can dominate gas phase reactive carbon in megacities

R. E. Dunmore[1], J. R. Hopkins[1,2], R. T. Lidster[1], J. D. Lee[1,2], M. J. Evans[1,2], A. R. Rickard[1,2], A. C. Lewis[1,2], and J. F. Hamilton[1]

[1]Wolfson Atmospheric Chemistry Laboratories, Department of Chemistry, University of York, Heslington, York, YO10 5DD, UK
[2]National Centre for Atmospheric Science, University of York, Heslington, York, YO10 5DD, UK

Correspondence to: J. Hamilton (jacqui.hamilton@york.ac.uk)

Abstract

Hydrocarbons are key precursors to two priority air pollutants, ozone and particulate matter. Those with two to seven carbons have historically been straightforward to observe and have been successfully reduced in many developed cities through air quality policy interventions. Longer chain hydrocarbons released from diesel vehicles are not considered explicitly as part of air quality strategies and there are few direct measurements of their gaseous abundance in the atmosphere. This study describes the chemically comprehensive and continuous measurements of organic compounds in a developed megacity (London), which demonstrate that on a seasonal median basis, diesel-related hydrocarbons represent only 20–30 % of the total hydrocarbon mixing ratio but comprise more than 50 % of the atmospheric hydrocarbon mass and are a dominant local source of secondary organic aerosols. This study shows for the first time that, 60 % of the winter primary hydrocarbon hydroxyl radical reactivity is from diesel-related hydrocarbons and using the maximum incremental reactivity scale, we predict that they contribute up to 50 % of the ozone production potential in London. Comparing real-world urban composition with regulatory emissions inventories in the UK and US highlights a previously unaccounted for, but very significant, under-reporting of diesel related hydrocarbons; an underestimation of a factor ~ 4 for C_9 species rising to a factor of over 70 for C_{12} during winter. These observations show that hydrocarbons from diesel vehicles can dominate gas phase reactive carbon in cities with high diesel fleet fractions. Future control of urban particulate matter and ozone in such locations requires a shift in policy focus onto gas phase hydrocarbons released from diesels as this vehicle type continues to displace gasoline world-wide.

1 Introduction

With an increasing proportion of the world's population living in cities, rising from only 3 % in the 1800's to over 47 % by the end of the 20th Century (Gaffney and Marley, 2009), the impact of urban air pollution has become a significant factor in global health (Harrison

et al., 2012). The costs of air pollution are high even in those locations that have seen considerable improvements in air quality over the past decades (Chameides et al., 1992); in the UK exposure to particulate matter (PM) alone is estimated to reduce life expectancy on average by around 7–8 months, with a cost to society estimated at up to GBP 20 billion per year (House of Commons Environmental Audit Committee, 2012).

Primary urban air pollution emissions are dominated by PM, nitrogen oxides (NO_x), carbon monoxide (CO) and volatile organic compounds (VOCs). Many of these species can react in the atmosphere to create secondary pollutants, such as ozone (O_3), oxygenated VOCs (OVOCs), peroxy acyl nitrates (PANs) and condensed materials in the form of secondary organic aerosol (SOA), which add to the overall PM load (Robinson et al., 2007; Atkinson and Arey, 2003; Odum et al., 1997).

Air quality in London has been controlled and monitored for over 60 years, making it in theory one of the better understood atmospheres of the world's megacities. Current measurements in London focus on assessing national compliance with legally prescribed air quality standards, and this includes the hydrocarbons 1,3-butadiene and benzene. However, compliance measurements in themselves are insufficient to fully describe the chemical and physical processes occurring in the urban atmosphere (McMeeking et al., 2012), and a particular weakness lies in speciating the many different classes of carbon compounds in urban air.

The past two decades have seen declining concentrations of most smaller hydrocarbons in European and US cities, a result of tighter regulation of sources such as vehicle exhaust, evaporation and solvents (von Schneidemesser et al., 2010; Warneke et al., 2012), better control of natural gas leakage and an overall switch from gasoline to diesel powered vehicles. Current national emissions estimates suggest that the bulk of organic emissions to air are associated with smaller hydrocarbons, and this has driven policy, regulation and observation strategies for compliance. Figure 1 shows Government-estimated emissions for the UK (left) and US (right), categorised into the dominant emission sources. It is clear that based on current emission inventories, gaseous organic emissions from diesel appear to represent a negligible fraction of reactive carbon released into the atmosphere. The de-

mand for diesel fuel is expected to increase by 75 % between 2010 and 2040 and by 2020 it is expected to overtake gasoline as the number one transport fuel used worldwide (Exxon Mobil, 2014). The environmental impacts of this change are evaluated in part based on the national emission inventories that underpin Fig. 1.

The efficiency with which O_3 and SOA can be formed from diesel or gasoline emissions is dependent on the mass of available organic carbon, and the reactivity and volatility of that material (Gros et al., 2007; Jimenez et al., 2009; Donahue et al., 2012). To quantify this requires individual speciation of VOCs in order that each property can be properly estimated. The key urban sources of organic compounds include combustion products, unburnt fuels and evaporative emissions of fuels and solvents, all of which are highly complex, often propagating the original complexity of fossil fuels into the air. Whilst each VOC has a unique set of reaction mechanisms, in general terms, as the carbon number increases, the relative complexity of reactions and yields of SOA and O_3 also increase (Hamilton and Lewis, 2003). The organic mixture in air is complicated further by the presence of secondary oxygenated products. This requires a combined approach to investigate VOC composition, such as using two different gas chromatography systems.

Several recent field studies have investigated the relative importance of gasoline, diesel and biogenic emissions in generating SOA (Gentner et al., 2012; Bahreini et al., 2012; Gordon et al., 2013; Platt et al., 2013; Gordon et al., 2014a, b; Jathar et al., 2014; Ensberg et al., 2014). These have been carried out predominately in the US, particularly in California, where current diesel usage is rather low by global standards. The US diesel fleet is dominated by heavy-duty vehicles, leading to a difference in the source strength of diesel and gasoline engines between weekdays and the weekend. In contrast, this trend is not observed in London (see Supplement and Fig. S1), which has a different vehicle fleet composition, with 60 % diesel fuel use, and a large number of diesel buses operating at similar times to domestic vehicles. It is also important to consider that London and Los Angeles (arguably the world's most well studied city for air pollution) have significant differences in terms of urban geography, population density, commuting patterns, amount of green space/trees and upwind sources (expanded in the Supplement and Table S1). Specif-

ically, the high population density in central London, and the fact that many vehicle journeys both begin and end in central London (rather than radial vehicle commuting); resulting in the central London atmosphere experiencing both cold and warm start vehicle emissions. Also worth noting is that there is no large upwind source of BVOCs in London, rather the natural emissions are distributed rather homogeneously across the city (Fig. S2).

This work uses high resolution VOC measurements to investigate the abundance and trends of diesel related hydrocarbons in the atmosphere at a typical urban background site in London. By comparison to the emission inventories, we highlight a severe underestimation in the impact of gaseous VOC emissions from diesel on urban air quality that is likely replicated across Europe and other cities globally where diesel vehicle use is high.

2 Experimental

2.1 Clean air for London campaign

Two 5 week campaigns were conducted as part of the National Environment Research Council (NERC) funded Clean Air for London (ClearfLo) project in January/February and July/August 2012 at an urban background site (see Fig. S3) based at Sion Manning School in North Kensington, London. For more information about this site and the ClearfLo project refer to Bigi and Harrison (2010) and Bohnenstengel et al. (2014) respectively.

2.2 Gas chromatography measurements

Two gas chromatography (GC) instruments were used during the ClearfLo campaign, a dual channel GC-flame ionisation detector (DC-GC-FID) and a comprehensive two dimensional GC (GC $\times$ GC-FID). Outside air was sampled from a manifold at 4 m from the ground through a condensation finger in an ethylene glycol bath held at $-30\,^{\circ}\mathrm{C}$, to remove any moisture from the sample. See Supplement for details about calibrations.

The DC-GC-FID was operated by the National Centre for Atmospheric Science (NCAS) Facility for Ground Atmospheric Measurements (FGAM) with the instrument set up and

calibration described in Hopkins et al. (2003). In brief, the system has three GC columns that operate in parallel, where after sampling and desorption the flow is split 50 : 50; one column is an aluminium oxide (Al_2O_3) Porous Layer Open Tubular (PLOT, 50 m, 0.53 mm id) for non-methane hydrocarbons (NMHCs) analysis; and the other column is actually two LOWOX columns in series (10 m, 0.53 mm id) for OVOC analysis.

The GC × GC-FID is comprised of a Markes TT24-7 thermal desorption (TD) unit with an air server attachment (Markes International, Llantrisant, UK) and an Agilent 7890 GC (Agilent Technologies, Wilmington, DE, USA) equipped with an FID operating at 200 Hz. The TD unit sampled at a rate of 100 mL min^{-1} for 55 min, giving a total sample volume of 5.5 L. The trap temperature was set to $-10\,^{\circ}C$, held for 3 min, then on injection heated at 100 °C min^{-1} to 200 °C to ensure all analytes of interest were desorbed.

The GC × GC-FID system first dimension column was a BPX-5 (25 m × 0.15 mm, 0.4 µm df), at 50 psi, combined with a second dimension column of a BP-20 (5 m × 0.25 mm, 0.25 µm df), at 23 psi (SGE, Australia), with column pressures controlled using the Agilent 7890 EPC. The total transfer flow valve modulator incorporated a 6-port, 2-way diaphragm valve (Valco Instruments, Houston, TX, USA), with actuation achieved using a solenoid valve, controlled by software written "in house". The modulator was held at 120 °C throughout the run and had a modulation period of 5 s, with 4.7 s sample and 0.3 s injection times. The chromatographic and modulation configuration of the GC × GC-FID system is detailed in Lidster et al. (2011). During the injection of sample, liquid carbon dioxide (CO_2) was sprayed onto the first 2 cm portion at the head of the first dimension column for 60 s to re-focus the sample.

An oven temperature programme was developed which optimised separation and resolution of compounds of interest. The initial oven temperature was 30 °C, held for 1 min, ramped at 2.5 °C min^{-1} to 130 °C, held for 1 min then ramped at 10 °C min^{-1} to 200 °C, and held for 1 min; giving a total run time of 50 min. This, combined with the TD run time, gave a total analysis time of 55 min.

During the summer campaign, some parameters had to be changed. Ambient temperatures were higher in comparison to the winter, meaning the oven temperature programme

had to be altered to allow the oven to reach its minimum temperature. The initial oven temperature was changed to 35 °C held for 2 min and the final temperature of 200 °C was held for 2 min. All other oven parameters were kept the same. Due to a sensitivity drop, the TD sampling rate was increased to 200 mL min^{-1} for 55 min, to give a total sample volume of 11 L.

2.3 Supporting measurements

Measurements of NO_x were made using a single channel, chemiluminesence instrument (Air Quality Design Inc., USA), which has a wide linear range (1 ppt to 500 ppb). Lee et al. (2009) Ozone measurements were made using an UV Absorption TEI 49C and 49i (Thermo Scientific) with a limit of detection of 1 ppb.

3 Observations of hydrocarbons in urban air

The two GC instruments individually quantified 78 VOCs (36 aliphatics, 19 monoaromatics, 21 oxygenated and 2 halogenated), as well as many hundreds more included in a lumped carbon number assessment from 2667 samples (1352 winter and 1315 summer). The DC-GC instrument measured volatile VOCs, C_1–C_7 hydrocarbons and a selection of OVOCs, with effective saturation concentrations (Nannoolal et al., 2004, 2008) ranging from 3×10^7 to 1.4×10^{12} µg m^{-3}. The GC × GC-FID instrument measured the less volatile VOC fraction (effective saturation concentration range of 1.8×10^6 to 2.4×10^9 µg m^{-3}), with hydrocarbons from C_6 to C_{13}, plus a large group of OVOCs (from C_3 onwards). There was some overlap in species measured by both instruments, with good agreement seen (e.g. benzene R^2 0.92, slope 1.070 ± 0.013, see Fig. S4).

The number of possible structural isomers increases exponentially with carbon number (Goldstein and Galbally, 2007) and beyond around C_9 it becomes impossible to accurately identify the structure of every hydrocarbon present in air. Using the retention behaviour of each compound on chromatographic columns it is however possible to assign individual species to particular chemical classes and functionalities. Here we group according to car-

bon number and basic functionality, an example of which can be seen in Fig. 2. The C_2-C_6 volatility range contains both primary hydrocarbon emissions, with isomers quantified individually, along with several oxygenated compounds. Between C_6 to C_{13}, a wide range of hydrocarbon and OVOC species, including the n-alkanes, α-pinene, limonene, monoaromatics with up to 3 substituents and naphthalene were quantified individually (see Fig. S5 and Table S2).

3.1 Grouping of unresolved complex mixtures

In previous studies using GC-FID, the larger hydrocarbon fraction, where diesel VOC emissions are predominately found, is part of an unresolved complex mixture (UCM). One method used to estimate the relative amounts of VOCs in this region, is to identify the *n*-alkane (which is often observed as a well defined peak above a raised baseline) and then integrate the area above the blank baseline between two consecutive linear alkanes (using an FID) or to use the *m/z* 57 fragment ion to represent primary intermediate VOC (IVOC) (Zhao et al. , 2014). In reality, this gives an estimate of the total or alkyl containing IVOC loading within this volatility range and will not only include the hydrocarbon fraction with that specific carbon number but other compounds as well (*i.e.* lower carbon number aromatics, OVOCs). This study details the improved resolution of VOCs using GC$\times$GC to allow for a more stringent grouping of the UCM by carbon number and functionality, rather than by volatility.

Higher carbon number aliphatic compounds (C_6-C_{13}, predominantly alkanes with some alkenes and cycloalkanes), C_4 substituted monoaromatics and C_{10} monoterpenes have been grouped together and the combined class abundance estimated using a response ratio to the corresponding straight-chained *n*-alkane, 1,3-diethyl benzene and α-pinene respectively. The group boundaries are shown in Fig. 2, where for example, box 7 corresponds to the C_{12} aliphatic group and encompasses alkanes, cyclic alkanes and alkenes. Only the material within the box is integrated within this retention window. This is a clear improvement over the 1D case, as there are a considerable number of peaks, with a higher 2^{nd} dimension retention time, in Fig. 2 that would co-elute with the aliphatic group if the en-

tire retention window was co-sampled (*i.e.* aromatics, oxygenates and other hetero atom containing species). The number of individual isomer peaks that could be isolated in the aliphatics grouping increased from 9 for the C_6 group to 40 for C_{10} (shown in Fig. 6, black squares). A full table of the observed isomer peaks and group mass concentrations is provided in Table S3.

Unfortunately, the separation of the linear alkanes, branched alkanes, cyclic aliphatic and alkenes on the GC×GC chromatogram is not sufficient at higher carbon numbers to allow them to be more fully resolved. This is a direct consequence of the use of the cryogen free and field deployable valve modulator, which when used in total transfer mode, where the flow in the first column slows during the modulation pulse, imposes restrictions on the column dimensions and internal diameters that can be used (Lidster et al., 2011). Also, given the temperature constraints on this instrument, it is likely that the GC×GC not only misses a fraction of the C_{13} aliphatic group but that may also be under-reporting the number of isomers in the higher carbon number groups. This would explain why the number of isomers decreases after C_{11} aliphatics, rather than increases as would be expected. The aliphatic groups have diurnal behaviour (discussed in the next section) that indicate a dominant traffic related source. Fuel composition measurements suggest there is unlikely to be significant quantities of alkenes from traffic related sources; gasoline contains around 3-4 wtC% of alkenes, and diesel contains negligible quantities (Gentner et al., 2012).

3.2 Diurnal behaviour

The average diurnal behaviour of a selection of VOCs, O_3 and NO_x, are shown in Fig. 3. VOCs with an anthropogenic source (e.g. ethane, toluene, C_4 substituted monoaromatics and C_{13} aliphatics) have higher mixing ratios in winter, consistent with reduced rates of photochemical removal in the northern European winter and a lower boundary layer height. Toluene and NO_x are strong indicators of traffic related emissions, and both have diurnal profiles with rush hour peaks, commonly observed in urban areas (Borbon et al., 2001; Parrish et al., 2009; Gaffron, 2012). The profiles of the higher carbon number species, C_4 substituted monoaromatics and C_{13} aliphatics, show similar traffic-related profiles, strongly

indicative that this is their major source. Those species with a dominant biogenic source (e.g. isoprene and α-pinene) are higher in summer, due to increased emission. The winter profiles of isoprene and α-pinene show possible anthropogenic sources, traffic and cleaning products respectively.

3.3 Reactivity and mass calculations of grouped compounds

Figure 4 shows the relative emission source contributions of compounds to the total hydrocarbon mixing ratio (top), mass concentration (middle) and primary hydrocarbon hydroxyl radical (OH) reactivity (bottom), calculated by carbon number, and split according to emission source. For each sample, the mass concentration ($\mu g\, m^{-3}$) and primary hydrocarbon OH reactivity (s^{-1}, see Supplementary Information Section 1.7 for explicit details on the calculation of OH reactivity) were calculated and a seasonal median calculated using the mixing ratios of the individual components and the summation of all further unidentified species within the ten class groups, not including the OVOCs. OH reactivity is defined as the total psuedo first order rate coefficient for loss of OH when reacting with VOCs in the atmosphere. This is important in urban atmospheres that are VOC limited, such as London, as the reaction of VOCs with the OH radical is the driving force for the formation of O_3 and other secondary pollutants.

The Passant (2002) speciated emissions inventory was used to determine the main emission sources for each compound. For C_2 to C_5, the main source is either natural gas usage or leakage, followed by road transport use. From C_6 onwards, the main emission source was classified as road transport or other fuel usage categories (i.e. filling of petrol stations). To determine the percentage contributions from diesel or gasoline fuel usage, the detailed fuel characterisation of Gentner et al. (2012) was used with a value of 60 % diesel use in the UK (Department of Energy and Climate Change, 2014).

Although the summer data has been shown throughout the remainder of the article, care should be taken when interpreting the impacts. It is likely that the summer observations are made up of '*residual*' VOCs remaining after transport from emission source and subsequent photochemical reactions. This could lead to a small overestimation of the contribution

of diesel-related hydrocarbons and an underestimation of some species, particularly the OVOCs.

The winter has generally higher abundances of hydrocarbons, with summer showing a marked increase in the biogenic source compounds. In both winter and summer, in mixing ratio terms, the distribution is dominated by high volatility species (over 85 % of the total) primarily from natural gas and gasoline sources. When viewed in terms of mass concentration, however, the distribution of combined natural gas and gasoline vs. diesel is closer to 70 : 30 % in winter and 77 : 23 % in summer, the latter due to the increased loss rates for reactive species in summer disproportionately removing larger hydrocarbons.

In order to calculate primary hydrocarbon OH reactivity of diesel emissions, rate constants have to be estimated as each individual species is not uniquely identified and because the rate constants (and subsequent chemistry) are un-measured in the majority of cases for hydrocarbons larger than C_8. The nearest straight-chain alkane rate constant (Atkinson and Arey, 2003) is applied to all carbon in that aliphatic grouping. This will lead to a conservative estimate of reactivity since cycloalkanes and alkenes would be expected to react faster (i.e. the k_{OH} for the reaction of *n*-dodecane is 1.32×10^{-11} cm^3 molecule^{-1} s^{-1}, compared to that of 1-dodecene which is 5.03×10^{-11} cm^3 molecule^{-1} s^{-1} (Aschmann and Atkinson, 2008), for further details see Supplementary Information Section 1.7 and Table S4). For the C_4 substituted monoaromatic and C_{10} monoterpene groups, the rate constants of 1,3 diethyl benzene and α-pinene respectively were used.

3.4 Calculation of unmeasured diesel emissions

The GC measurements stop at C_{13}, however diesel typically has a range of hydrocarbons from C_9 to C_{22} that peaks with *n*-hexadecane as the most abundant compound. Using the observed distribution of $C_{10}-C_{13}$, allows for an estimate to be made of the remaining, *unobserved* NMHC fraction of gaseous diesel emissions in the $C_{14}-C_{22}$ range, using the fuel composition-based emission factors for the gas phase compounds from Gentner et al. (2013). Assuming no atmospheric loss, a reasonable approximation in winter, it is estimated that the GC $\times$ GC-FID technique observes around 25–30 % of the total gaseous

hydrocarbon emissions from diesel sources. It is then possible to estimate a seasonal average unmeasured gas phase NMHC mass concentration from diesel sources in London as 76.1–97.8 $\mu g\,m^{-3}$ in winter and 26.8–34.3 $\mu g\,m^{-3}$ in summer. These values can be compared to typical primary organic aerosol measurements of 1 $\mu g\,m^{-3}$ (Zhang et al., 2011; Young et al., 2015), indicating that, in ambient air, diesel-related emission of hydrocarbons are overwhelmingly (a factor of 100) to the gas phase, consistent with laboratory and tail pipe studies Gordon et al. (2013). In contrast, using gasoline liquid fuel speciation, the combined GC approach can observe approximately over 98 % of the mass of gasoline.

The impact of the unobserved diesel emissions on primary hydrocarbon OH reactivity was estimated using the *n*-dodecane rate constant as a proxy. The percentage contributions to mixing ratio (top), mass concentration (middle) and primary hydrocarbon OH reactivity (bottom), divided by emission source, including the unmeasured diesel emissions and OVOCs, are shown in Fig. 5. It is clear that diesel plays an important role in the composition of NMHCs and their subsequent reactivity. The total (measured + calculated) diesel emissions contribute 5.1 and 1.7 s^{-1} to OH reactivity in winter and summer respectively compared to 1.7 and 0.8 s^{-1} from gasoline compounds; increasing the contribution of diesel-related hydrocarbons to calculated VOC OH reactivity from 23 % using the measured VOCs to 61 % including the unmeasured I/VOCs in winter and from 8 to 34 % in summer (full details can be found in Table S5). In summer, the primary emissions have undergone a degree of loss due to photochemical ageing and so the values are an underestimate of the fuel sources. These diesel-related hydrocarbons may be partly responsible for the "missing" OH reactivity observed between measurements of OH lifetime vs. the value calculated from observed sinks in many studies (Yoshino et al., 2006, 2012).

3.5 Comparison to emissions inventories

Assuming that: the winter observations are made "at source" (hence atmospheric losses and lifetime differences can be neglected), the measurement location is representative of an urban setting, and the UK inventory correctly estimates the emission for toluene (based on direct flux comparisons made in London by Langford et al., 2010), there appears to be

a significant inventory under-reporting for the higher carbon number species. When normalising to toluene, the UK national emissions inventory, which is believed to use best-practice international reporting methodologies, underreports by a factor of 4.6 for C_9 species, rising to a factor of 74 for C_{12} compounds (see Fig. 6). Given the clear traffic diurnal profiles of the $C_{10}-C_{13}$ species (seen in Fig. 3m for C_{13} aliphatics), which essentially encompasses only diesel fuel, the most likely source of these species is gaseous emissions from the diesel vehicle fleet, either evaporative, tailpipe or a combination of the two. These observations provide the first direct evidence of significant diesel hydrocarbons in London's ambient air, something that could previously only be inferred from liquid fuel measurements and exhaust studies.

3.6 Ozone formation potentials

At present, there is insufficient kinetic and mechanistic data to allow for the accurate modelling of the impact diesel hydrocarbons will have on photochemical ozone. Unlike Los Angeles, which is typically impacted by intense single-day episodic photochemical ozone events, in London (and NW Europe), higher ozone levels are usually the result of regional-scale multi-day formation. Therefore, different control strategies and reactivity scales, which take into account trans-boundary transport, have been developed and applied in Europe. Photochemical ozone creation potentials (POCPs, e.g. Derwent et al., 1998) have been derived using idealized 5 day photochemical trajectory model runs over Europe, incorporating detailed chemical degradation schemes of the emitted VOCs (Saunders et al., 2003). Individual POCP values depend upon emissions along the trajectory, the reactivity of the VOC and its propensity to form ozone, i.e. the number of C-C and C-H bonds in the reactive species. Calvert et al., (2008), using the Master Chemical Mechanism (MCMv3.1, http://mcm.leeds.ac.uk/MCM) and speciated emission inventories (Passant, 2002), with little speciation of alkanes above C_9, found that alkanes dominated POCP-weighted emissions (33 %) on the regional scale in Europe, accounting for slightly more than the aromatics (29 %) and significantly more than the alkenes (20 %) and oxygenates (17 %) (Calvert et al., 2000). They also note that this is in marked contrast with that found on the urban scale in

Los Angeles, where alkanes contribute little to the intense episodic ozone formation observed. The work presented here shows that emission inventories severely underestimate the amount of alkanes emitted from diesel sources, hence these have are not been included in previous studies on ozone formation. Based on the POCP results of Calvert et al. (2000) for shorter chain alkanes, and considering the high OH reactivity of larger hydrocarbons, incorporating the diesel related aliphatics into future calculations is likely to have a significant impact on regional ozone formation in Europe, and likely elsewhere.

However, despite the lack of chemical information available, we can make an assessment of the effects that the new diesel VOC observations have on local ozone productivity by calculating the O_3 Formation Potential (OFP) of each emission source using a Maximum Incremental Reactivity (MIR) scale, as determined by Carter (2010) using the SAPRC-07 mechanism. The MIR scale is based upon one-day photochemical simulations in a box moving over an urban basin and subject to ozone precursor emissions. The NO_x concentrations are adjusted so that the final ozone concentration in a simulation showed the maximum sensitivity to changes in emissions of organic compounds, these conditions give the MIR. MIRs represent relatively high NO_x conditions, often experienced in US cities, where control of the emissions of VOCs is the most effective means of reducing ozone formation (Carter, 2010).

MIR values for a range of important VOC emission classes (alkanes, alkenes, aromatics, oxygenates) compare well to POCP values calculated using detailed MCMv3.1 chemistry in a one day US urban photochemical trajectory model, giving us confidence in the tuned SAPRC-07 chemistry for predicting photochemical ozone formation under typical one-day high NO_x, high ozone conditions (Derwent et al., 2010). However, caution must be observed when applying MIR scales to other conditions (i.e. NW Europe), as previously discussed.

For those species included in one of the carbon number and functionality VOC groups, a weighted MIR value has been calculated assuming a composition of 95 % branched alkane and 5 % alkene. The calculated, unobserved diesel emissions were given a MIR value based on the weighted contributions of the different compound classes from the diesel fuel gaseous emission speciation in Gentner et al. (2013).

The calculated OFP values for summer and winter are shown in Fig. 7, with a clear seasonal difference in the importance of different emission sources. The winter is dominated by emissions from diesel (over 45 ± 4.6 %). In contrast, the summer shows a marked increase in contribution from oxygenated species, rising from 18 % in winter to 40 % in summer. Gentner et al. (2013) concluded that gasoline emissions contributed the majority of potential O_3 formation, however given that gasoline is the primary fuel used in the US (quoted at 73–90 % of total fuel use; Gentner et al., 2012) this is not surprising. Whereas in the UK, diesel fuel accounts for an average of 60 % of total fuel use and as such would be expected to contribute a larger percent towards O_3 formation.

Given that many of the higher carbon number species, likely emitted from the combustion of diesel, are not currently included in emissions inventory and as such are missing from many model chemical mechanisms (e.g. MCMv3.3.1), a more rigorous reactivity analysis is not possible (e.g. POCPs discussed previously). It is possible to infer from this analysis however, that as winter diesel emissions contribute nearly 50 % of the OFP and over 60 % of primary hydrocarbon OH reactivity, it is likely that they would have a large impact on the overall reactivity and chemistry of the urban atmosphere.

3.7 Potential impacts on SOA formation

Over the last few years, there has been robust debate in the literature over the relative importance of diesel vs. gasoline for SOA production, arising in part because of the difficulties of measuring diesel hydrocarbon emissions (Ensberg et al., 2014; Gordon et al., 2014a, b; Platt et al., 2013; Bahreini et al., 2012). Recent studies have shown the unspeciated emissions from combustion sources lead to significantly more SOA production than those that can be speciated by conventional instrumentation. Jathar et al. (2014), used simulation chamber data and source-specific SOA yield parameterizations for these unspeciated emissions to estimate that, in the US, 90 % of SOA was from biomass burning and gasoline sources, with 85 % of the SOA coming from unspeciated organic emissions.

There is a clear need to improve measurements of larger hydrocarbons that represent a large part of what is referred to in other studies as unspeciated chemicals. In this study,

the uncertainty in the unspeciated fraction has been reduced by grouping ambient observations of VOCs by carbon number and functionality. The $> C_9$ aliphatic groups are dominated by diesel emissions at this location and so the SOA source strength can be more accurately determined. The potential contributions of the higher hydrocarbons to SOA formation has been estimated by multiplying the median measured VOC mass concentration (Fig. 8, top panel, black columns) by the corresponding SOA yield (Fig. 8, top panel, blue circles) (Zhang et al., 2014). The yields applied were measured in high NO_x chamber studies (VOC_0/NO_x (ppbC ppb^{-1}) of 0.5) with an organic aerosol mass C_{OA} of 10 µg m^{-3}, representative of urban areas (Zhang et al., 2014; Presto et al., 2010). Here it is assumed that NMHCs with less than six carbons and aqueous chemistry of water soluble oxidation products, such as glyoxal, do not contribute to SOA mass (Knote et al., 2014). In both winter and summer, the observed levels of aliphatic compounds from diesel sources have the potential to form significant quantities of SOA (Fig. 8, bottom panel, red columns). If a diesel SOA yield of 0.15 is applied to the total diesel emissions (as calculated previously), then gas phase emissions from diesel engines represent the dominant traffic related precursor source of urban SOA in a European megacity such as London, where the use of diesel fuel is prevalent, in line with previous studies in the US (Gentner et al., 2012). Each cubic meter of air contains sufficient gas phase hydrocarbons to potentially produce 14.4–17.6 and 4.9–6.1 µg of SOA in winter and summer following atmospheric oxidation.

Recent simulation chamber studies indicate that modern engines fitted with diesel particle filters, such as EURO5 emissions control, have greatly reduced VOC tailpipe emission and form little SOA under chamber conditions (Gordon et al., 2014a, b). However, Carslaw and Rhys-Tyler (2013) have recently shown that when vehicles are driven under real-world urban conditions (*i.e.* different engines loads cause variable catalyst temperatures which can lead to limited effectiveness, as opposed to dynamometer tests where the catalyst is held at optimum operating conditions), the emission of NO_x from diesel engines have not been reduced as expected given the new technologies implemented. It is possible to infer that if NO_x emissions are higher than expected, the VOC emissions are also likely to be

higher. In this study we have shown that there is a significant diesel vehicle source emitting sufficient VOCs to impact ozone and SOA formation in the urban atmosphere.

4 Conclusions

From the results presented, it is possible to conclude that current inventories and emissions estimates do not adequately represent emissions of gas phase higher carbon number species from the diesel fleet under real-world conditions and in a developed urban environment. The calculated impact of these species is significant, particularly in terms of OH reactivity, ozone formation potential and SOA production.

In the last decade, there has been a steady shift in fuel use in many locations. For example, in the UK diesel fuel use as a fraction of total fuel has risen from 52 % in 2005 to 62 % in 2011 (see Fig. S7 and Table S7) (Department of Energy and Climate Change, 2014). Although the UK may be considered typical of Europe (where diesel use varies between 45–80 %) (European Commission, 2012), the average US value was around 29 % diesel use (U.S. Energy Information Administration, 2014) in 2013, with the understanding of other geographical regions currently being poor.

This shift to an increasingly diesel-powered fleet in many developed cities, as a response to energy efficiency drivers, has therefore shifted the balance of hydrocarbons in urban air from short to long chain compounds, and these observations provide direct atmospheric evidence of this effect in London. Previous air quality assessments of diesel-related hydrocarbons in the atmosphere are few in number, and as discussed previously, have been made only in the US where geographic characteristics and vehicle fleet composition are very different to London, and Europe more widely. In many cities the impact of diesel hydrocarbons remains to be determined, but this work demonstrates that it will likely be significant in locations with substantial diesel fleets. An improvement in measurement infrastructure appears to be essential if this source is to be quantified more widely or the impacts of policy evaluated.

Understanding the impact of this change is significantly hindered however by a lack of appropriate physico-chemical data for individual longer chain hydrocarbons. There are already very significant policy challenges for many developed cities relating to the control of NO_2 from modern diesel vehicles, and this study indicates that there may also be a similar, but currently un-recognized, policy challenge to control reactive carbon emissions and their contributions to secondary pollutants.

The Supplement related to this article is available online at doi:10.5194/acpd-0-1-2015-supplement.

Author contributions. R. E. Dunmore and J. R. Hopkins analysed the GC data and J. D. Lee made the O_3 and NO_x measurements. R. T. Lidster and J. F. Hamilton developed the GC $\times$ GC-FID instrument. A. R. Rickard provided insight into the kinetics and photochemical ozone creation potentials. R. E. Dunmore, J. F. Hamilton, A. C. Lewis and M. J. Evans wrote the paper. All authors contributed towards the final version of the paper.

Acknowledgements. R. E. Dunmore would like to thank NERC (NE/J500197/1) for PhD funding and to acknowledge David Carslaw for his assistance using Openair and Richard Derwent for assistance with the NAEI. All authors would like to acknowledge NERC for funding the Clearflo project (NE/H002112/1), and the efforts of all participants in the field experiment in supporting these measurements. We would like to acknowledge Stephen Belcher for project co-ordination.

References

Aschmann, S. and Atkinson, R.: Rate constants for the gas-phase reactions of OH radicals with E-7-tetradecene, 2-methyl-1-tridecene and the C_7–C_{14} 1-alkenes at 295 ± 1 K, Phys. Chem. Chem. Phys., 10, 4159–4164, doi:10.1039/B803527J, 2008.

Atkinson, R. and Arey, J.: Atmospheric degradation of volatile organic compounds, Chem. Rev., 103, 4605–4638, doi:10.1021/cr0206420, 2003.

Bahreini, R., Middlebrook, A., de Gouw, J., Warneke, C., Trainer, M., Brock, C., Stark, H., Brown, S., Dube, W., Gilman, J., Hall, K., Holloway, J., Kuster, W., Perring, A., Prévôt, A., Schwarz, J.,

Spackman, J., Szidat, S., Wagner, N., Weber, R., Zotter, P., and Parrish, D.: Gasoline emissions dominate over diesel in formation of secondary organic aerosol mass, Geophys. Res. Lett., 39, doi:10.1029/2011GL050718, 2012.

Bigi, A. and Harrison, R.: Analysis of the air pollution climate at a central urban background site, Atmos. Environ., 44, 2004–2012, doi:10.1016/j.atmosenv.2010.02.028, 2010.

Bohnenstengel, S. I., Belcher, S. E., Aiken, A., Allan, J. D., Allen, G., Bacak, A., Bannan, T. J., Barlow, J., Beddows, D. C. S., Bloss, W. J., Booth, A. M., Chemel, C., Coceal, O., Di Marco, C. F., Dubey, M. K., Faloon, K. H., Fleming, Z. L., Furger, M., Gietl, J. K., Graves, R. R., Green, D. C., Grimmond, C. S. B., Halios, C. H., Hamilton, J. F., Harrison, R. M., Heal, M. R., Heard, D. E., Helfter, C., Herndon, S. C., Holmes, R. E., Hopkins, J. R., Jones, A. M., Kelly, F. J., Kotthaus, S., Langford, B., Lee, J. D., Leigh, R. J., Lewis, A. C., Lidster, R. T., Lopez-Hilfiker, F. D., McQuaid, J. B., Mohr, C., Monks, P. S., Nemitz, E., Ng, N. L., Percival, C. J., Prévôt, A. S. H., Ricketts, H. M. A., Sokhi, R., Stone, D., Thornton, J. A., Tremper, A. H., Valach, A. C., Visser, S., Whalley, L. K., Williams, L. R., Xu, L., Young, D. E. E., and Zotter, P.: Meteorology, air quality, and health in London: the ClearfLo project, B. Am. Meteorol. Soc., online first, doi:10.1175/bams-d-12-00245.1, 2014.

Borbon, A., Fontaine, H., Veillerot, M., Locoge, N., Galloo, J., and Guillermo, R.: An investigation into the traffic-related fraction of isoprene at an urban location, Atmos. Environ., 35, 3749–3760, doi:10.1016/S1352-2310(01)00170-4, 2001.

Calvert, J. G., Derwent, R. G., Orlando, J. J., Tyndall, G. S., and Wallington, T. J.: Mechanisms of Atmospheric Oxidation of the Alkenes; Oxford University Press: New York, 2000.

Carslaw, D. and Rhys-Tyler, G.: New insights from comprehensive on-road measurements of NO_x, NO_2 and NH_3 from vehicle emission remote sensing in London, UK, Atmos. Environ., 81, 339–347, doi:10.1016/j.atmosenv.2013.09.026, 2013.

Carslaw, D. and Ropkins, K.: openair – an R package for air quality data analysis, Environ. Modell. Softw., 27–28, 52–61, doi:10.1016/j.envsoft.2011.09.008, 2012a.

Carslaw, D. and Ropkins, K.: openair – data analysis tools for the Air Quality Community, The R Journal, 4, 20–29, 2012b.

Carter, W.: SAPRC-07 Atmospheric Chemistry Mechanisms and VOC Reactivity Scales, available at: http://www.engr.ucr.edu/~carter/SAPRC/ (last access: 10 February 2015), 2010.

Chameides, W., Fehsenfeld, F., Rodgers, M., Cardelino, C., Martinez, J., Parrish, D., Lonneman, W., Lawson, D., Rasmussen, R., Zimmerman, P., Greenberg, J., Middleton, P., and Wang, T.: Ozone

precursor relationships in the ambient atmosphere, J. Geophys. Res.-Atmos., 97, 6037–6055, doi:10.1029/91JD03014, 1992.

Department of Energy and Climate Change: Road transport energy consumption at regional and local authority level, available at: www.gov.uk/government/statistical-data-sets/road-transport-energy-consumption-at-regional-and-local-authority-level (last access: 10 February 2015), 2014.

Derwent, R., Jenkin, M., Saunders, S., and Pilling, M.: Photochemical ozone creation potentials for organic compounds in northwest Europe calculated with a master chemical mechanism, Atmos. Environ., 32, 2429–2441, doi:10.1016/S1352-2310(98)00053-3, 1998.

Derwent, R., Jenkin, M., Pilling, M., Carter, W., and Kaduwela, A.: Reactivity scales as comparative tools for chemical mechanisms, J. Air Waste Manage., 60, 914–924, doi:10.3155/1047-3289.60.8.914, 2010.

Donahue, N. M., Kroll, J. H., Pandis, S. N., and Robinson, A. L.: A two-dimensional volatility basis set – Part 2: Diagnostics of organic-aerosol evolution, Atmos. Chem. Phys., 12, 615–634, doi:10.5194/acp-12-615-2012, 2012.

Ensberg, J., Hayes, P., Jimenez, J., Gilman, J., Kuster, W., de Gouw, J., Holloway, J., Gordon, T., Jathar, S., Robinson, A., and Seinfeld, J.: Emission factor ratios, SOA mass yields, and the impact of vehicular emissions on SOA formation, Atmos. Chem. Phys., 14, 2383–2397, doi:10.5194/acp-14-2383-2014, 2014.

European Commission: EU Transport in Figures, available at: http://ec.europa.eu/transport/facts-fundings/statistics/doc/2012/pocketbook2012.pdf (last access: 10 February 2015), 2012.

Exxon Mobil: The Outlook for Energy: A view to 2040, Tech. rep., Exxon Mobil Corporation, Texas, 2014.

Gaffney, J. and Marley, N.: The impacts of combustion emissions on air quality and climate – from coal to biofuels and beyond, Atmos. Environ., 43, 23–36, doi:10.1016/j.atmosenv.2008.09.016, 2009.

Gaffron, P.: Urban transport, environmental justice and human daily activity patterns, Transport Policy, 20, 116–129, 12th World Conference on Transport Research (WCTR)/14th World Conference of the Air-Transport-Research-Society (ATRS), Lisbon, Portugal, 11–15 July 2010, 2012.

Gentner, D., Isaacman, G., Worton, D., Chan, A., Dallmann, T., Davis, L., Liu, S., Day, D., Russell, L., Wilson, K., Weber, R., Guha, A., Harley, R., and Goldstein, A.: Elucidating secondary organic aerosol from diesel and gasoline vehicles through detailed characterization of organic carbon emissions, P. Natl. Acad. Sci. USA, 109, 18318–23, doi:10.1073/pnas.1212272109, 2012.

Gentner, D., Worton, D., Isaacman, G., Davis, L., Dallmann, T., Wood, E., Herndon, S., Goldstein, A., and Harley, R.: Chemical composition of gas-phase organic carbon emissions from motor vehicles and implications for ozone production, Environ. Sci. Technol., 47, 11837–11848, doi:10.1021/es401470e, 2013.

Goldstein, A. and Galbally, I.: Known and unexplored organic constituents in the Earth's atmosphere, Environ. Sci. Technol., 41, 1514–1521, doi:10.1021/es072476p, 2007.

Gordon, T., Tkacik, D., Presto, A., Zhang, M., Jathar, S., Nguyen, N., Massetti, J., Truong, T., Cicero-Fernandez, P., Maddox, C., Rieger, P., Chattopadhyay, S., Maldonado, H., Maricq, M. M., and Robinson, A.: Primary gas- and particle-phase emissions and secondary organic aerosol production from gasoline and diesel off-road engines, Environ. Sci. Technol., 47, 14137–14146, doi:10.1021/es403556e, 2013.

Gordon, T. D., Presto, A. A., May, A. A., Nguyen, N. T., Lipsky, E. M., Donahue, N. M., Gutierrez, A., Zhang, M., Maddox, C., Rieger, P., Chattopadhyay, S., Maldonado, H., Maricq, M. M., and Robinson, A. L.: Secondary organic aerosol formation exceeds primary particulate matter emissions for light-duty gasoline vehicles, Atmos. Chem. Phys., 14, 4661–4678, doi:10.5194/acp-14-4661-2014, 2014a.

Gordon, T. D., Presto, A. A., Nguyen, N. T., Robertson, W. H., Na, K., Sahay, K. N., Zhang, M., Maddox, C., Rieger, P., Chattopadhyay, S., Maldonado, H., Maricq, M. M., and Robinson, A. L.: Secondary organic aerosol production from diesel vehicle exhaust: impact of aftertreatment, fuel chemistry and driving cycle, Atmos. Chem. Phys., 14, 4643–4659, doi:10.5194/acp-14-4643-2014, 2014b.

Gros, V., Sciare, J., and Yu, T.: Air-quality measurements in megacities: focus on gaseous organic and particulate pollutants and comparison between two contrasted cities, Paris and Beijing, CR Geosci., 339, 764–774, doi:10.1016/j.crte.2007.08.007, 2007.

Hamilton, J. and Lewis, A.: Monoaromatic complexity in urban air and gasoline assessed using comprehensive GC and fast GC-TOF/MS, Atmos. Environ., 37, 589–602, doi:10.1016/S1352-2310(02)00930-5, 2003.

Harrison, R. M., Dall'Osto, M., Beddows, D. C. S., Thorpe, A. J., Bloss, W. J., Allan, J. D., Coe, H., Dorsey, J. R., Gallagher, M., Martin, C., Whitehead, J., Williams, P. I., Jones, R. L., Langridge, J. M., Benton, A. K., Ball, S. M., Langford, B., Hewitt, C. N., Davison, B., Martin, D., Petersson, K. F., Henshaw, S. J., White, I. R., Shallcross, D. E., Barlow, J. F., Dunbar, T., Davies, F., Nemitz, E., Phillips, G. J., Helfter, C., Di Marco, C. F., and Smith, S.: Atmospheric chemistry and physics in the atmosphere of a developed megacity (London): an overview of the REPARTEE

experiment and its conclusions, Atmos. Chem. Phys., 12, 3065–3114, doi:10.5194/acp-12-3065-2012, 2012.

Hopkins, J., Lewis, A., and Read, K.: A two-column method for long-term monitoring of non-methane hydrocarbons (NMHCs) and oxygenated volatile organic compounds (OVOCs), J. Environ. Monitor., 5, 8–13, doi:10.1039/b202798d, 2003.

House of Commons Environmental Audit Committee: Air Quality: A Follow-up Report, Ninth Report, Tech. rep., House of Commons, London, The Stationery Office Limited, 2012.

Jathar, S., Gordon, T., Hennigan, C., Pye, H. T., Pouliot, G., Adams, P., Donahue, N., and Robinson, A.: Unspeciated organic emissions from combustion sources and their influence on the secondary organic aerosol budget in the United States, P. Natl. Acad. Sci. USA, 111, 10473–10478, doi:10.1073/pnas.1323740111, 2014.

Jimenez, J. L., Canagaratna, M. R., Donahue, N. M., Prevot, A. S. H., Zhang, Q., Kroll, J. H., DeCarlo, P. F., Allan, J. D., Coe, H., Ng, N. L., Aiken, A. C., Docherty, K. S., Ulbrich, I. M., Grieshop, A. P., Robinson, A. L., Duplissy, J., Smith, J. D., Wilson, K. R., Lanz, V. A., Hueglin, C., Sun, Y. L., Tian, J., Laaksonen, A., Raatikainen, T., Rautiainen, J., Vaattovaara, P., Ehn, M., Kulmala, M., Tomlinson, J. M., Collins, D. R., Cubison, M. J. E., Dunlea, J., Huffman, J. A., Onasch, T. B., Alfarra, M. R., Williams, P. I., Bower, K., Kondo, Y., Schneider, J., Drewnick, F., Borrmann, S., Weimer, S., Demerjian, K., Salcedo, D., Cottrell, L., Griffin, R., Takami, A., Miyoshi, T., Hatakeyama, S., Shimono, A., Sun, J. Y., Zhang, Y. M., Dzepina, K., Kimmel, J. R., Sueper, D., Jayne, J. T., Herndon, S. C., Trimborn, A. M., Williams, L. R., Wood, E. C., Middlebrook, A. M., Kolb, C. E., Baltensperger, U., and Worsnop, D. R.: Evolution of Organic Aerosols in the Atmosphere, Science, 326, 1525–1529, doi:10.1126/science.1180353, 2014.

Knote, C., Hodzic, A., Jimenez, J. L., Volkamer, R., Orlando, J. J., Baidar, S., Brioude, J., Fast, J., Gentner, D. R., Goldstein, A. H., Hayes, P. L., Knighton, W. B., Oetjen, H., Setyan, A., Stark, H., Thalman, R., Tyndall, G., Washenfelder, R., Waxman, E., and Zhang, Q.: Simulation of semi-explicit mechanisms of SOA formation from glyoxal in aerosol in a 3-D model, Atmos. Chem. Phys., 14, 6213–6239, doi:10.5194/acp-14-6213-2014, 2014.

Langford, B., Nemitz, E., House, E., Phillips, G. J., Famulari, D., Davison, B., Hopkins, J. R., Lewis, A. C., and Hewitt, C. N.: Fluxes and concentrations of volatile organic compounds above central London, UK, Atmos. Chem. Phys., 10, 627–645, doi:10.5194/acp-10-627-2010, 2010.

Lee, J. D., Moller, S. J., Read, K. A., Lewis, A. C., Mendes, L., and Carpenter, L. J.: Year-round measurements of nitrogen oxides and ozone in the tropical North Atlantic marine boundary layer, J. Geophys. Res.-Atmos., 114, D21302, doi:10.1029/2009JD011878, 2009.

Lidster, R., Hamilton, J., and Lewis, A.: The application of two total transfer valve modulators for comprehensive two-dimensional gas chromatography of volatile organic compounds, J. Sep. Sci., 34, 812–821, doi:10.1002/jssc.201000710, 2011.

McMeeking, G. R., Bart, M., Chazette, P., Haywood, J. M., Hopkins, J. R., McQuaid, J. B., Morgan, W. T., Raut, J.-C., Ryder, C. L., Savage, N., Turnbull, K., and Coe, H.: Airborne measurements of trace gases and aerosols over the London metropolitan region, Atmos. Chem. Phys., 12, 5163–5187, doi:10.5194/acp-12-5163-2012, 2012.

Nannoolal, Y., Rarey, J., Ramjugernath, D., and Cordes, W.: Estimation of pure component properties: Part 1. Estimation of the normal boiling point of non-electrolyte organic compounds via group contributions and group interactions, Fluid Phase Equilibr., 226, 45–63, doi:10.1016/j.fluid.2004.09.001, 2004.

Nannoolal, Y., Rarey, J., and Ramjugernath, D.: Estimation of pure component properties: Part 3. Estimation of the vapor pressure of non-electrolyte organic compounds via group contributions and group interactions, Fluid Phase Equilibr., 269, 117–133, doi:10.1016/j.fluid.2008.04.020, 2008.

Odum, J. R., Jungkamp, T. P. W., Griffin, R. J., Forstner, H. J. L., Flagan, R. C., and Seinfeld, J. H.: Aromatics, reformulated gasoline, and atmospheric organic aerosol formation, Environ. Sci. Technol., 31, 1890–1897, doi:10.1021/es960535l, 1997.

Parrish, D., Kuster, W., Shao, M., Yokouchi, Y., Kondo, Y., Goldan, P. D., de Gouw, J., Koike, M., and Shirai, T.: Comparison of air pollutant emissions among mega-cities, Atmos. Environ., 43, 6435–6441, doi:10.1016/j.atmosenv.2009.06.024, 2009.

Passant, N.: Speciation of UK emissions of non-methane volatile organic compounds, Tech. rep., AEA Technology Report ENV-05452002, Culham, Abingdon, UK, 2002.

Platt, S. M., El Haddad, I., Zardini, A. A., Clairotte, M., Astorga, C., Wolf, R., Slowik, J. G., Temime-Roussel, B., Marchand, N., Ježek, I., Drinovec, L., Močnik, G., Möhler, O., Richter, R., Barmet, P., Bianchi, F., Baltensperger, U., and Prévôt, A. S. H.: Secondary organic aerosol formation from gasoline vehicle emissions in a new mobile environmental reaction chamber, Atmos. Chem. Phys., 13, 9141–9158, doi:10.5194/acp-13-9141-2013, 2013.

Presto, A., Miracolo, M., Donahue, N., and Robinson, A.: Secondary organic aerosol formation from high-NO_x photo-oxidation of low volatility precursors: n-alkanes, Environ. Sci. Technol., 44, 2029–2034, doi:10.1021/es903712r, 2010.

Robinson, A., Donahue, N., Shrivastava, M., Weitkamp, E., Sage, A., Grieshop, A., Lane, T., Pierce, J., and Pandis, S.: Rethinking Organic Aerosols: Semivolatile Emissions and Photochemical Aging, Science, 315, 1259–1262 doi:10.1126/science.1133061, 2007.

R Development Core Team: R: A Language and Environment for Statistical Computing, R Foundation for Statistical Computing, Vienna, Austria, available at: http://www.R-project.org/ (last access: 19 June 2014), 2012.

Saunders, S. M., Jenkin, M. E., Derwent, R. G., and Pilling, M. J.: Protocol for the development of the Master Chemical Mechanism, MCM v3 (Part A): tropospheric degradation of non-aromatic volatile organic compounds, Atmos. Chem. Phys., 3, 161–180, doi:10.5194/acp-3-161-2003, 2003.

U.S. Energy Information Administration: Petroleum and Other Liquids, 2014.

von Schneidemesser, E., Monks, P., and Plass-Duelmer, C.: Global comparison of VOC and CO observations in urban areas, Atmos. Environ., 44, 5053–5064, doi:10.1016/j.atmosenv.2010.09.010, 2010.

Warneke, C., de Gouw, J., Holloway, J., Peischl, J., Ryerson, T., Atlas, E., Blake, D., Trainer, M., and Parrish, D.: Multiyear trends in volatile organic compounds in Los Angeles, California: five decades of decreasing emissions, J. Geophys. Res.-Atmos., 117, D00V17, doi:10.1029/2012JD017899, 2012.

Yoshino, A., Sadanaga, Y., Watanabe, K., Kato, S., Miyakawa, Y., Matsumoto, J., and Kajii, Y.: Measurement of total OH reactivity by laser-induced pump and probe technique – comprehensive observations in the urban atmosphere of Tokyo, Atmos. Environ., 40, 7869–7881, doi:10.1016/j.atmosenv.2006.07.023, 2006.

Yoshino, A., Nakashima, Y., Miyazaki, K., Kato, S., Suthawaree, J., Shimo, N., Matsunaga, S., Chatani, S., Apel, E., Greenberg, J., Guenther, A., Ueno, H., Sasaki, H., Hoshi, J., Yokota, H., Ishii, K., and Kajii, Y.: Air quality diagnosis from comprehensive observations of total OH reactivity and reactive trace species in urban central Tokyo, Atmos. Environ., 49, 51–59, doi:10.1016/j.atmosenv.2011.12.029, 2012.

Young, D. E., Allan, J. D., Williams, P. I., Green, D. C., Flynn, M. J., Harrison, R. M., Yin, J., Gallagher, M. W., and Coe, H.: Investigating the annual behaviour of submicron secondary inorganic and organic aerosols in London, Atmos. Chem. Phys., 15, 6351–6366, doi:10.5194/acp-15-6351-2015, 2015.

Zhang, Q., Jimenez, J., Canagaratna, M., Ulbrich, I., Ng, N., Worsnop, D., and Sun, Y.: Understanding atmospheric organic aerosols via factor analysis of aerosol mass spectrometry: a review, Anal. Bioanal. Chem., 401, 3045–3067, doi:10.1007/s00216-011-5355-y, 2011.

Zhang, X., Cappa, C., Jathar, S., McVay, R., Ensberg, J., Kleeman, M., and Seinfeld, J.: Influence of vapor wall loss in laboratory chambers on yields of secondary organic aerosol, P. Natl. Acad. Sci. USA, 111, 5802–5807, doi:10.1073/pnas.1404727111, 2014.

Zhao, Y., Hennigan, C., May, A., Tkacik, D., de Gouw, J., Gilman, J., Kuster, W., Borbon, A., and Robinson, A.: Intermediate-Volatility Organic Compounds: A large source of Secondary Organic Aerosol, Environ. Sci. Technol., 48, 13743–137, doi:10.1021/es5035188, 2014.

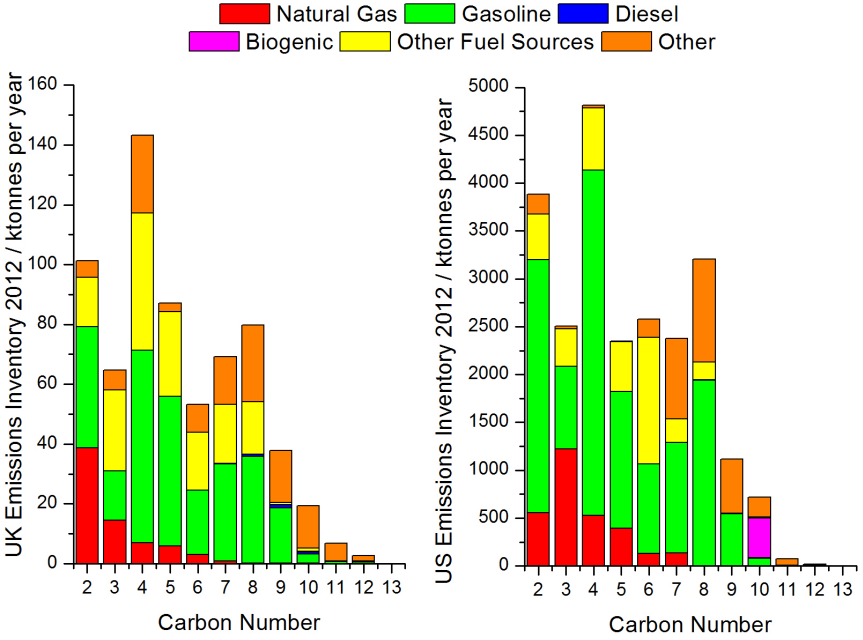

Figure 1. Total mass by carbon number and functionality from UK 2012 (left) and US 2011 (right) emission inventories. The carbon number and functionality of emissions have been estimated by applying the speciated inventory of emission sources of Passant (2002) to the most recent estimates of non-methane hydrocarbon source apportionment for each country (full details can be found in the Supplement).

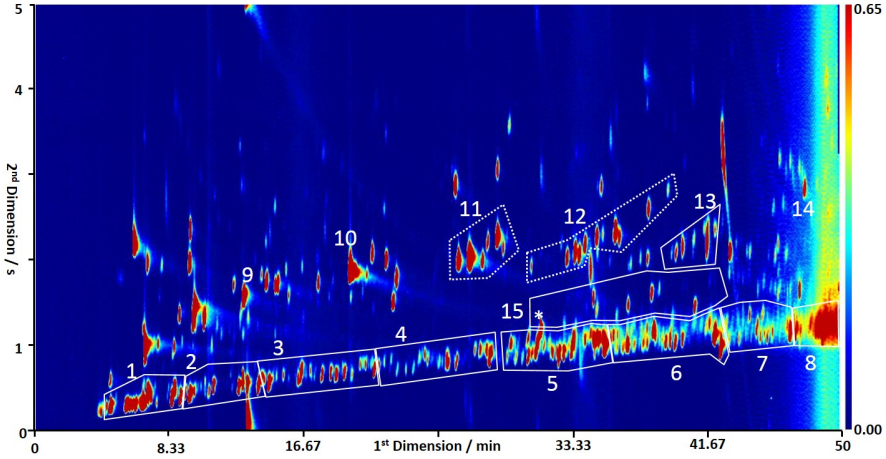

Figure 2. Typical GC×GC-FID chromatogram from 2012-07-25, demonstrating the grouping of compounds. The retentions on the first and second columns are the x and y axis respectively, with the intensity of the compound shown by the coloured contours. Labelled peaks and groups are identified as follows, with the dashed and solid lines indicating compounds that were identified individually and as a group respectively; (1-8) aliphatic groups from C_6 to C_{13}, (9) benzene, (10) toluene, (11) C_2 substituted monoaromatics, (12) C_3 substituted monoaromatics, (13) C_4 substituted monoaromatics, (14) naphthalene, and (15) C_{10} monoterpenes with * corresponding to α-pinene which is the start of that group. The remaining compounds, not enclosed in a box contain hetero-atoms, primarily oxygenates. The grouping of compounds was accomplished using the lasso technique in Zoex GC image software (Zoex, USA). This technique allows the software to calculate the area of all peaks included in the lasso.

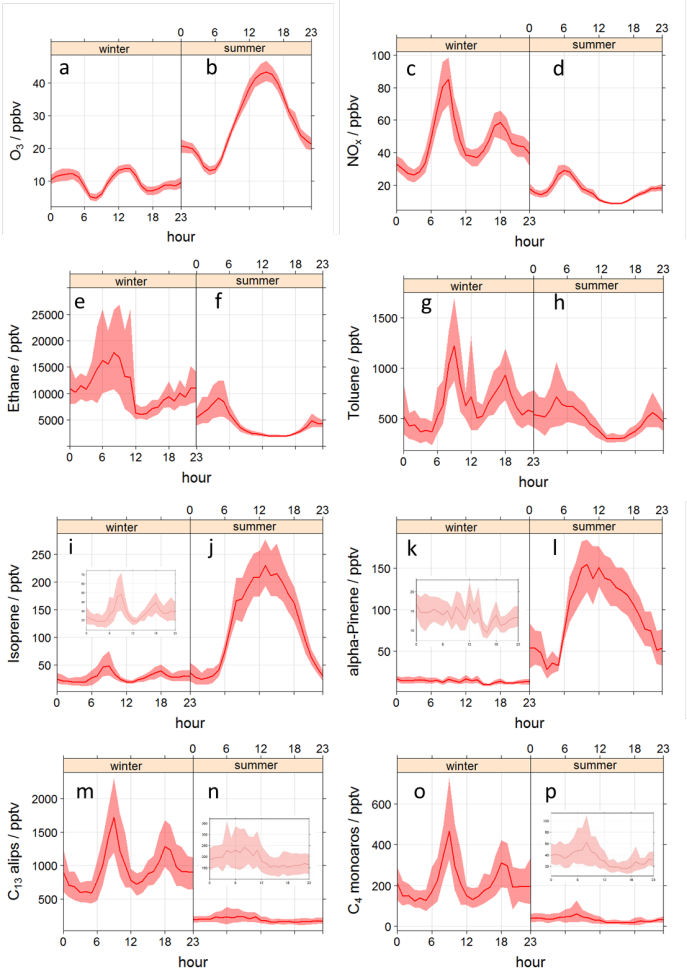
winter
summer
a
b
c
d
e
f
g
h
i
j
k
l
m
n
o
p
O_3 / ppbv
NO_x / ppbv
Ethane / pptv
Toluene / pptv
Isoprene / pptv
alpha-Pinene / pptv
C_{13} alips / pptv
C_4 monoaros / pptv
hour

Figure 3. Diurnal profiles of selected urban pollutants in winter (left-hand side of each plot) and summer (right-hand side of each plot). Winter and summer are plotted on the same y axes to show seasonal differences, with insets allowing the profile to be easily seen. (**a** and **b**) Ozone ($n = 2915$ and 2880; winter and summer, respectively), (**c** and **d**) nitrogen oxides ($n = 2915$ and 2880), (**e** and **f**) ethane ($n = 660$ and 681), (**g** and **h**) toluene ($n = 660$ and 680), (**i** and **j**) isoprene ($n = 660$ and 681), (**k** and **l**) α-pinene ($n = 691$ and 634), (**m** and **n**) C_{13} aliphatics ($n = 692$ and 632), (**o** and **p**) C_4 substituted monoaromatics ($n = 692$ and 563). Figure 3 was constructed using the OpenAir project for R where the solid line represents the mean daily concentration and the shaded regions shows the 95 % confidence intervals surrounding the mean (Carslaw and Ropkins, 2012a, b; R Development Core Team, 2012).

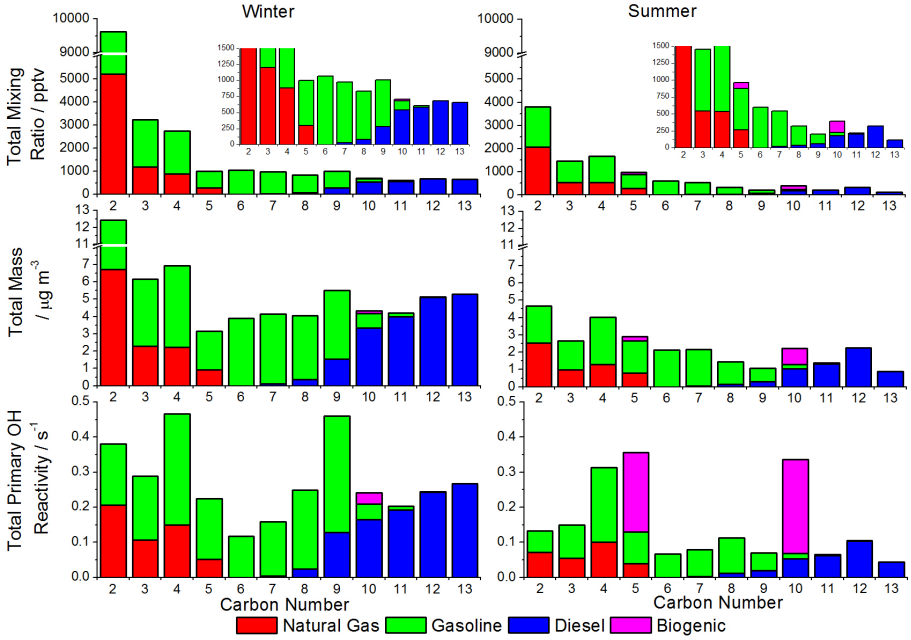

Figure 4. Seasonal median values for hydrocarbon mixing ratio, mass concentration and primary hydrocarbon OH reactivity in London air grouped by carbon number and potential emission source.

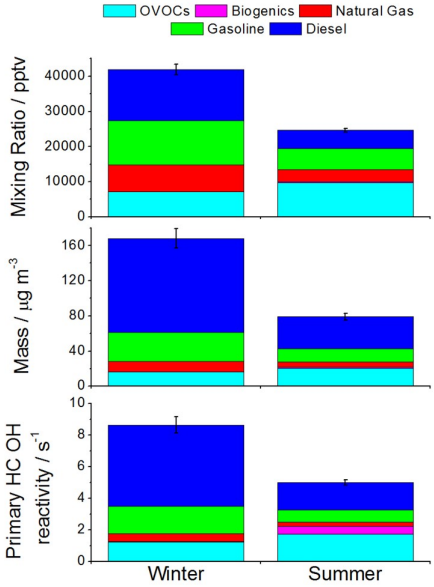

Figure 5. Contributions of emission source to total mixing ratio, mass and OH reactivity for winter and summer. Diesel is the summation of measured and calculated, with error bars indicating the uncertainty of the unobserved diesel NMHC fraction.

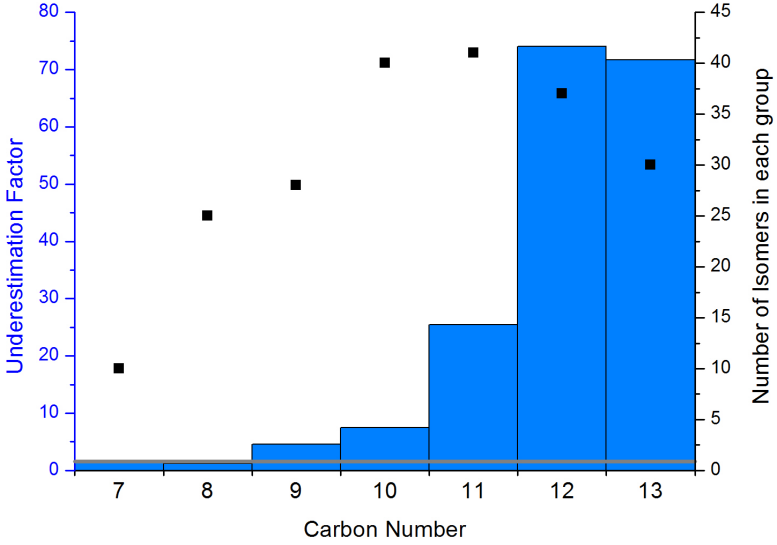

Figure 6. Winter emissions inventory underestimation (left axis and blue columns) and the number of isomers included in each grouped set of compounds (right axis and black squares). Grey line shows a factor of 1 *i.e.* inventory emission estimation is consistent with the observations.

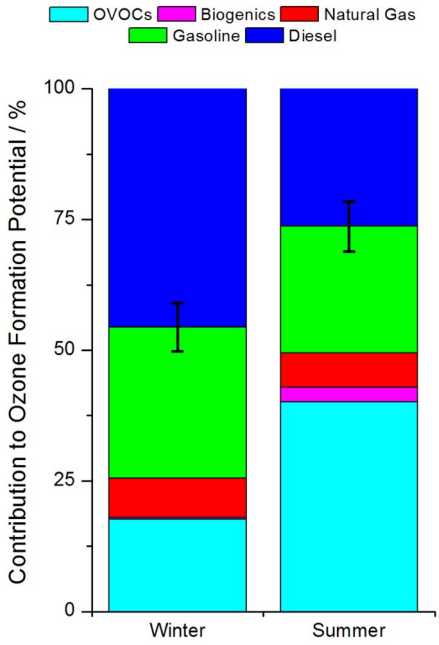

Figure 7. Contribution of emission sources to ozone formation potential, where diesel is representative of total diesel emissions and the error bars show the uncertainty of the unobserved diesel fraction calculation.

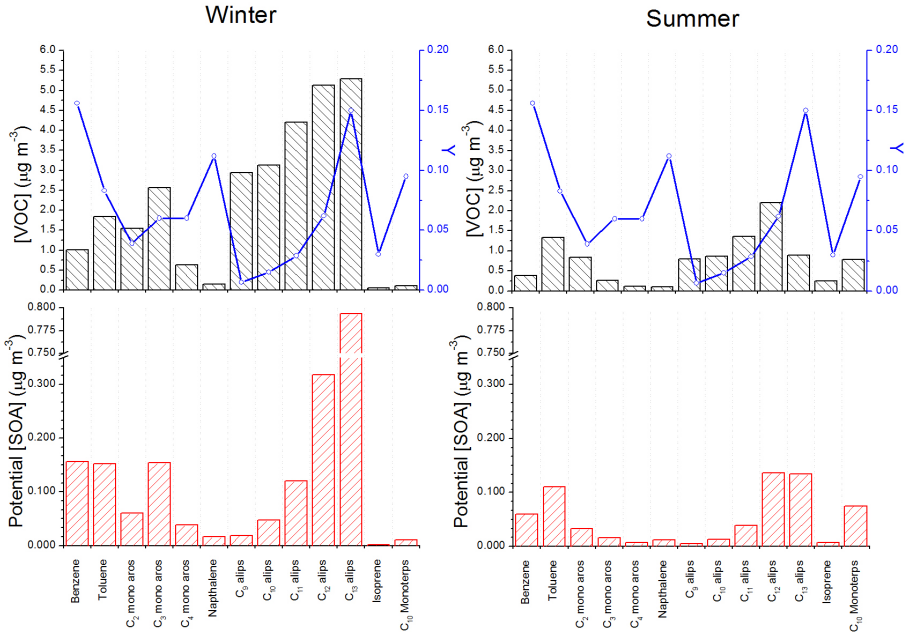

Figure 8. Potential SOA mass estimates. Upper: Mean VOC mass concentration [VOC] shown by black columns, and the corresponding SOA yields (Y) for the VOC precursors in blue circles. Lower: potential SOA mass concentration [SOA], calculated as the product of mean VOC mass and SOA yields. Winter shown on left and summer shown on right hand side panels.